Special Issue

Collagen Structural Changes in Rat Tarsus After Crosslinking

Sruti S. Akella[1,*], Juan Liu[1,2], Yuan Miao[1,3], Roy S. Chuck[1], Anne Barmettler[1], and Cheng Zhang[1]

[1] Department of Ophthalmology and Visual Sciences, Albert Einstein College of Medicine, Montefiore Medical Center, Bronx, NY, USA
[2] Department of Ophthalmology, Ning Xia Eye Hospital, Yinchuan, China
[3] Aier School of Ophthalmology, Central South University, Changsha, China

Correspondence: Cheng Zhang, Department of Ophthalmology and Visual Sciences, Montefiore Medical Center, 3332 Rochambeau Avenue, Centennial Building, Third Floor, Bronx, NY 10467, USA. e-mail: chzhang@montefiore.org
Anne Barmettler, Department of Ophthalmology and Visual Sciences, Montefiore Medical Center, 3332 Rochambeau Avenue, Centennial Building, Third Floor, Bronx, NY 10467, USA. e-mail: annebarmettler@gmail.com

Purpose: Surgery is the standard treatment for floppy eyelid syndrome, but crosslinking (CXL) tarsus has recently been proposed as an alternative. To the best of our knowledge, this study is the first to use second-harmonic generation (SHG) microscopy to examine tarsal collagen ex vivo before and after photo-activated crosslinking. To quantify crosslinking, this study examined fluorescence recovery after photobleaching (FRAP), which indirectly measures tissue stiffness.

Methods: Upper eyelid tarsal plates were dissected from 21 Sprague–Dawley rats (total of 42 tarsal plates). Six normal plates were sent for histopathology and SHG imaging; the remaining 36 were crosslinked with phosphate-buffered saline (PBS) alone or riboflavin in PBS (concentrations of 0.1%, 0.3%, and 0.5%). Tissues were irradiated with 365-nm ultraviolet A light (power, 0.45 mW/cm^2) for 30 minutes and immediately underwent SHG microscopy. Stiffness was indirectly measured with FRAP using fluorescein isothiocyanate (FITC)–dextran.

Results: SHG imaging of normal tarsus showed that the organization of collagen bundles is complex and varies greatly depending on location. After crosslinking with high-concentration riboflavin (0.5%), collagen fibers showed clear structural changes, becoming more densely packed and wavier compared to control. FRAP half-time to fluorescence recovery was significantly increased ($P < 0.05$), indirectly indicating increased tissue stiffness. No structural changes were observed after crosslinking with lower riboflavin concentrations of 0.1% and 0.3%.

Conclusions: This is the first report of SHG microscopy used to image tarsus collagen before and after crosslinking. These results highlight collagen structural changes, with effects on tissue stiffness indirectly confirmed by FRAP.

Translational Relevance: Collagen fibers in the tarsus may be a therapeutic target for crosslinking in order to treat symptomatic floppy eyelid syndrome.

Introduction

Eyelid tarsus is a complex biomechanical tissue that serves as the main support for the eyelid.[1] Structural alterations in the tarsus can cause various disease conditions such as entropion, ectropion, and floppy eyelid syndrome (FES). These can, in turn, lead to intense patient discomfort, ocular surface complications, and loss of vision. These acquired disorders are thought to be a result of alterations in collagen and elastin, which are the major components of the tarsal plate.[1]

The current conventional treatment for FES is surgical; a large piece of tarsus is removed in order to tighten the upper eyelid and prevent eversion. However, the recurrence rate after surgical resection may be as high as 40%.[2] Furthermore, many patients with floppy eyelid syndrome suffer from obstructive sleep apnea, metabolic syndrome, or high blood pressure, all of which may make for a poor surgical candidate.[2] In these patients, a nonsurgical treatment could be optimal.

Recently, tarsal crosslinking (CXL), or the process of forming strong covalent bonds between neighboring collagen fibrils, has been explored in animal and

cadaver models as an alternative treatment to stiffen tarsus in FES.[3–6] Crosslinking is already well known to most ophthalmologists as a treatment for keratoconic corneas. In the US Food and Drug Administration-approved Dresden protocol, corneas incubated with riboflavin are exposed to ultraviolet A (UV-A) radiation. The process generates reactive oxygen species that crosslink collagen fibers and ultimately stiffen the cornea, halting the ectatic process. Because crosslinking ultimately works by creating bonds between collagen, hypothetically any collagen-rich structure could also be targeted. To this point, the theory behind tarsus crosslinking arises from previous histopathological studies of floppy eyelids that showed that collagen fibers accumulate as elastin degrades.[7,8] This is likely a compensatory mechanism by which excess collagen is produced in order to counteract overload, prevent fatigue, and resist the abnormal force generated by an increasingly floppy eyelid. Theoretically, tarsal crosslinking would target and strengthen this excess collagen, thereby alleviating symptoms of FES. If this is the case, crosslinking should alter the microstructure of collagen, and indeed Zyablitskaya et al.[9] showed that scleral CXL is seen microscopically as increased "waviness" of collagen fibers.

To test the efficacy of CXL, previous papers have focused on histopathological and tensile load studies of the tarsus; however, conventional histopathology requires a certain amount of tissue processing. Extrapolating from the work done by Li et al.,[10] this processing may potentially alter tissue at a microscopic level. Ideally, a method to examine the tissue without staining or fixation would be used. One such method is second-harmonic generation (SHG) microscopy, which is a coherent nonlinear process in which two incident photons interact with tissue at a specific plane and are directly converted into a single photon without absorption or emission. Computer software is able to capture this conversion at different planes and generate a three-dimensional image of collagen fibers. Without tissue staining or fixation, the collagen fibers can be viewed ex vivo with minimal tissue manipulation.

In this study, SHG microscopy was used to image rat tarsus collagen before and after photo-activated crosslinking. Finally, SHG microscopy was coupled with a separate technique called fluorescence recovery after photobleaching (FRAP), which measures the diffusion of fluorescently tagged molecules within live tissues and has been shown previously to correlate with tissue stiffness in mouse sclera.[11,12] We hypothesized that SHG is a more sensitive measurement of CXL effects and therefore will detect changes at lower energy levels than other described techniques.

Methods

A total of 42 upper eyelid tarsal plates were harvested from 21 Sprague–Dawley rats. The rat was chosen as the experimental model for two reasons: fresh tissue is readily available from the rat, and the layers of the rat eyelid histologically appear similar to those of the human eyelid.[13] Six of these specimens were immediately sent for conventional histopathology ($n = 3$) or imaging with SHG microscopy ($n = 3$) as normal control. The remaining 36 tarsal plates were randomly crosslinked using control (PBS) and one of three riboflavin concentrations. We chose 0.1% as the starting concentration because it is the same solution used in the Dresden corneal protocol. Using this as a starting point, we hypothesized that the tarsus would require a stronger concentration compared to the cornea, so 0.3% and 0.5% concentrations were added. Then, 20 tarsal plates were sent for SHG imaging and FRAP; 16 tarsal plates were examined with histopathology (Fig. 1). All animal experiments adhered to the ARVO Statement for the Use of Animals in Ophthalmic and Vision Research.

Sample Preparation

Twenty-one Sprague–Dawley rats (Charles River Laboratories, Wilmington, MA) were euthanized at 6 weeks of age, and a total of 42 upper eyelids were immediately harvested en bloc from the medial to the lateral canthus. To isolate tarsal plates for study, the lids were dissected to remove the skin and orbicularis, along with the attachments of the levator aponeurosis and Müller's muscle, without altering the posterior conjunctiva. The lid margin with skin and hair follicles was left untouched (Fig. 2). Irradiation and imaging took place within 3 hours after euthanasia.

Irradiation

Individual tarsal plates were soaked in either PBS (control) or one of three different concentrations (0.1%, 0.3%, or 0.5%) of riboflavin (riboflavin 5′-phosphate salt hydrate powder; Merck KGaA, Darmstadt, Germany) in PBS for 30 minutes. Next the tarsal plates were exposed to a beam of UV-A radiation (Analytik Jena, Jena, Germany) with a peak wavelength of 365 nm at a distance of 5 cm. The total radiation density of the UV-A light source was measured 5 cm away from the light source with two independent meters, the NeuLog UV sensor (Eisco Scientific LLC, Victor, NY) and the General Tools Digital UVA/UVB
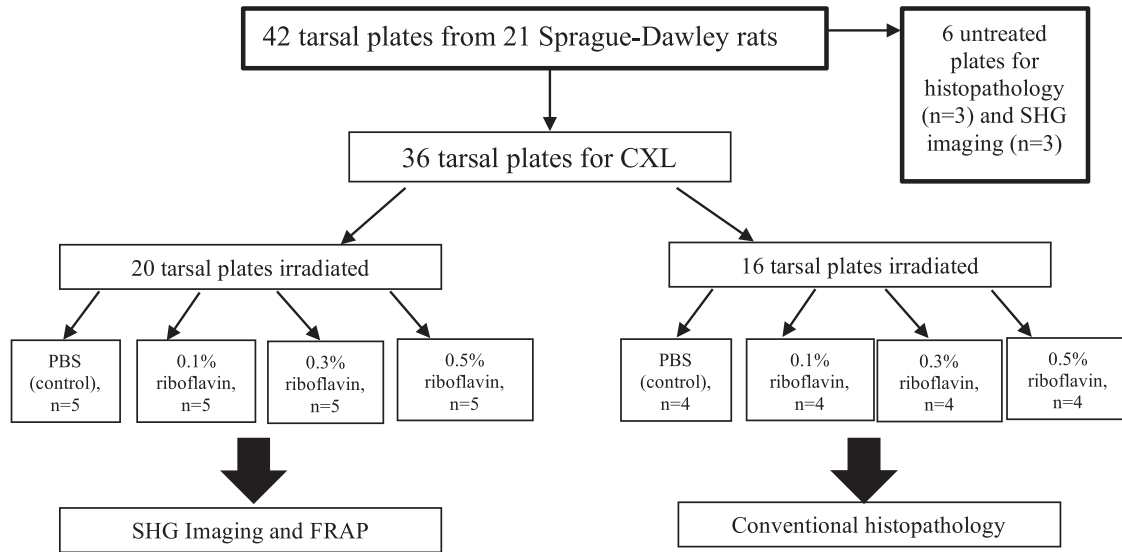
```
                  ┌─────────────────────────────────────────────┐        ┌───────────────────┐
                  │  42 tarsal plates from 21 Sprague-Dawley rats │───────▶│   6 untreated     │
                  └─────────────────────────────────────────────┘        │   plates for      │
                                        │                                 │  histopathology   │
                                        ▼                                 │  (n=3) and SHG    │
                  ┌─────────────────────────────────────────────┐        │  imaging (n=3)    │
                  │          36 tarsal plates for CXL             │        └───────────────────┘
                  └─────────────────────────────────────────────┘
```

20 tarsal plates irradiated				16 tarsal plates irradiated			
PBS (control), n=5	0.1% riboflavin, n=5	0.3% riboflavin, n=5	0.5% riboflavin, n=5	PBS (control), n=4	0.1% riboflavin, n=4	0.3% riboflavin, n=4	0.5% riboflavin, n=4
SHG Imaging and FRAP				Conventional histopathology			

Figure 1. Flowchart illustrating how specimens were processed.
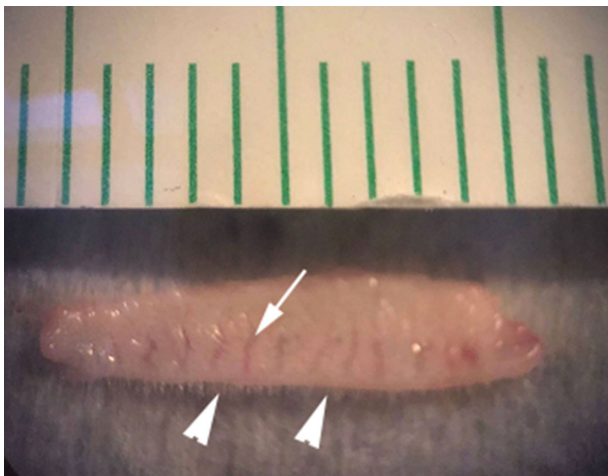

Figure 2. A rat tarsal plate from the upper eyelid with conjunctival epithelium and lid margin. Each division on the ruler represents 1 mm. *Arrow*, Meibomian gland; *arrowheads*, eyelid margin.

Meter (General Tools Manufacturing Co., Inc., New York, NY), and found to be 0.45 mW/cm^2. The tissue was then washed with PBS for 20 seconds. After irradiation, all tarsal plates were soaked in fluorescein isothiocyanate (FITC)–dextran solution (FD-40, 1 mg/mL, molecular weight 40 kDa; Sigma-Aldrich, St. Louis, MO) in the dark for 30 minutes. The protocol was adapted from Smith et al.[3]

SHG Imaging and FRAP Study

Second-harmonic generation images were generated with an inverted Olympus IX81 two-photon excited fluorescence microscope (FluoView FV-1000; Olympus Corporation of the Americas, Central Valley, PA).

The methodology was adapted from prior work done by Marando et al.[14] and Park et al.[15,16] To obtain images, the tarsal plate was placed on a glass-bottom plate (Thermo Fisher Scientific, Waltham, MA) with the posterior (conjunctival) side facing downward and coverslipped with 20 μL of FITC–dextran solution. A two-photon laser (titanium:sapphire) was tuned to 840 nm and directed through a dichroic mirror (RDM690; Olympus). A 25×, NA 1.05 water immersion objective was used to focus the excitation beam and collect backscatter signals. The SHG signal was collected through a bandpass emission filter (425/30 nm) after reflection by a dichroic mirror (DM458; Olympus). A square image (512 × 512 μm) was acquired at a resolution of 1024 × 1024 pixels in approximately 15 seconds, and multiple, consecutive, image stacks (z-stacks) were acquired using the same objective lens. When images were z-stacked, samples were scanned in 1-μm steps in the z-axis. For reference, the 0-μm position in depth corresponds to the first z-position where the SHG signal is detected. All images were obtained at a depth of 30 μm, which was chosen because preliminary experiments showed the clearest images of collagen fibers at this depth, where the fibers were most regularly arranged. This plane was determined to be ideal for analysis of collagen waviness.

After SHG scanning, FRAP imaging was performed on the same sample at the same tissue depth (30 μm). FRAP was performed by photobleaching fluorescent molecules at a specified location in tissue and monitoring the rate at which the bleached molecules were replaced by unbleached ones.[17] This rate, known as the fluorescence recovery time, was calculated by comparing the percentage of mobile and

immobile fractions to produce a half-time of bleach recovery ($t_{1/2}$), which was then used as the primary outcome measure:

$$I_{norm}(t) = \frac{I(t) - I_{bkg}(t)}{I_{prebleach} - I_{bkg}(t)} \times \frac{T_{prebleach} - I_{bkg}(t)}{T(t) - I_{bkg}(t)} \quad (1)$$

where I is the intensity of fluorescence signal at time t, I_{bkg} is the background intensity, $I_{prebleach}$ is the intensity prior to photobleaching, and T is the intensity of an unrelated, unbleached region, which is used as a reference in the image. The recovery curve was fitted by an exponential function to extract the half time of the recovery curve:

$$I(t) = (1 - e^{-t/\tau}) + I_0 I(t) = (1 - e^{-t/\tau}) + I_0 \quad (2)$$

$$t_{1/2} = -\frac{\ln 0.5}{\tau} t_{1/2} = -\frac{\ln 0.5}{\tau} \quad (3)$$

FRAP imaging data were collected using the same Olympus IX81 microscope with its argon 488-nm laser set at 5% power, 500 to 530 bandpass filter, and the plan apochromat 25×, NA 1.05 water objective lens. The imaging window was 512 × 512 µm, and the bleach zone was a circular disk 30 µm in diameter. Data collection consisted of three pre-scans at 5% power and a 488-nm laser followed by 100 iterations of 100% and 405-nm laser power directed at the bleach zone and then by 78 more full scans taken at 5% power and with a 488-nm laser during the following 40 seconds.

Here, the FRAP technique was used to measure the diffusion of FITC–dextran molecules. Measured diffusion was an indicator of permeability to small molecules in the tarsal plates, which could then be correlated to amount of stiffness. In each region, four geographic zones were examined and the results were recorded. These regions were chosen randomly from one of four imaginary quadrants. The intensities in each bleached region of interest were measured using the ImageJ FRAP Profiler tool (National Institutes of Health, Bethesda, MD).

Histopathology

After the tarsal plates were soaked in riboflavin and irradiated as described above, specimens were fixed in formalin for 72 hours and embedded in paraffin. Cross-sections (5 µm) were cut along the vertical meridian and stained with hematoxylin and eosin for histopathological study.
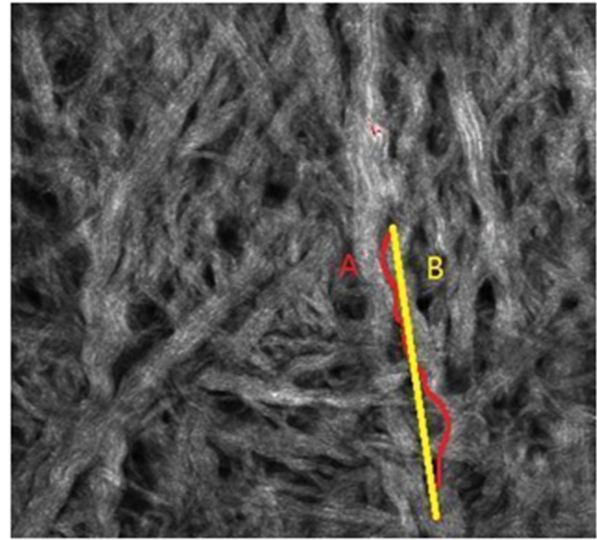

Figure 3. Sample SHG microscopy image at a depth of 30 µm showing how collagen waviness was analyzed: ratio of length A/length B, measured with ImageJ software (lines A and B end at the same point; line B overlaps line A at the inferior portion). Original magnification, 400×.

Collagen Waviness Analysis

For quantitation of collagen fiber waviness from the SHG images, each collagen fiber was traced along its entire length using ImageJ. Waviness was calculated as a ratio of the length of the traced fiber to the length of a straight path between the end points (Fig. 3). This was done for 10 randomly selected fibers in each tarsal plate, a methodology adapted from prior work.[9,18,19] From the experimental area (512 × 512 µm), these fibers were chosen randomly, separated by a set distance. The investigator analyzing the images was masked to the riboflavin concentration.

Statistical Analysis

Data were reported as the mean ± standard deviation and analyzed using SPSS Statistics 24.0 (IBM, Armonk, NY). Each treated group was compared to the untreated control group, using independent sample *t*-tests. The statistical significance of all tests was defined as $P < 0.05$.

Results

Normal Eyelid and Tarsal Tissue Histology in Rats

Similar to the human eyelid, the normal rat eyelid consists of five layers: epidermis, dermis, orbicularis
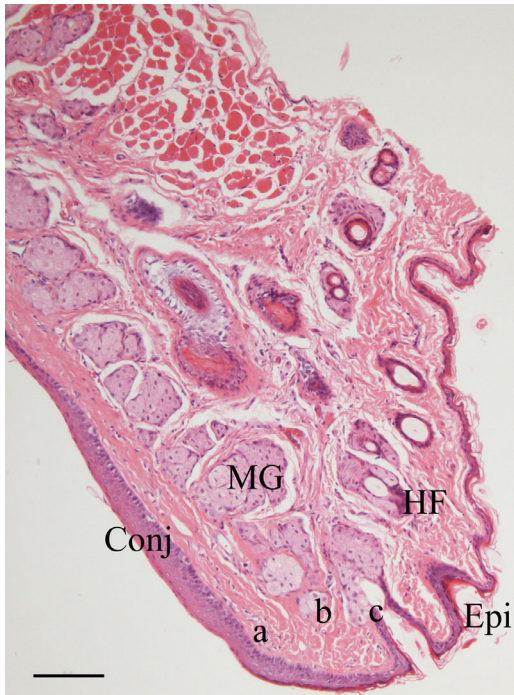
Figure 4. Histology of normal rat dissected tarsal plate and conjunctival epithelium with hair follicles at the lid margin. From left to right, the tarsal plate shows conjunctival epithelium (Conj), Meibomian glands (MG), a few hair follicles (HF), and epidermis (Epi). Lowercase labels a, b, and c indicate where SHG images were obtained (see Fig. 5). Hematoxylin and eosin stain. Original magnification, 200×. *Scale bar*: 100 μm.

Figure 5. SHG images of a normal tarsal plate demonstrate the different arrangements of collagen bundles at different locations. The images (A, B, and C) were taken at the corresponding lowercase locations identified in Figure 4 (a, b, c). (A) Connective tissue layer of the tarsal plate, just anterior to the conjunctival epithelium. This is a dense collagen structure with most collagen bundles arranged perpendicular to the lid margin. (B) Within the tarsus, Meibomian glands (*asterisks*) are interspersed with collagen bundles, which run parallel to the glands. (C) At the lid margin, a hair follicle (*arrow*) is surrounded by very thin, densely packed collagen bundles, which transition to bigger, straighter collagen bundles. All photographs were taken at a depth of 30 μm. *Scale bar*: 100 μm.

muscle, tarsus (dense connective tissue surrounding Meibomian glands), and palpebral conjunctiva. For crosslinking, the tarsal plate (Fig. 2) was harvested with the overlying conjunctival epithelium and hair follicles at the lid margin. The areas marked with a, b, and c in Figure 4 show the areas used to generate the SHG images in Figure 5.

SHG Imaging of Normal Tarsus

These SHG images of normal rat tarsus were taken at the corresponding locations marked with lowercase a, b, and c in Figure 4. The tarsus immediately anterior to the conjunctival epithelium is composed predominantly of dense collagen bundles arranged perpendicular to the lid margin. These bundles are relatively uniform in size (Fig. 5A). In Figure 5B, large empty spaces represent Meibomian glands, which are seen intermingled with collagen bundles. Closer to the epidermis, a hair follicle is surrounded by thin collagen bundles (Fig. 5C). This was found consistently in all control samples.
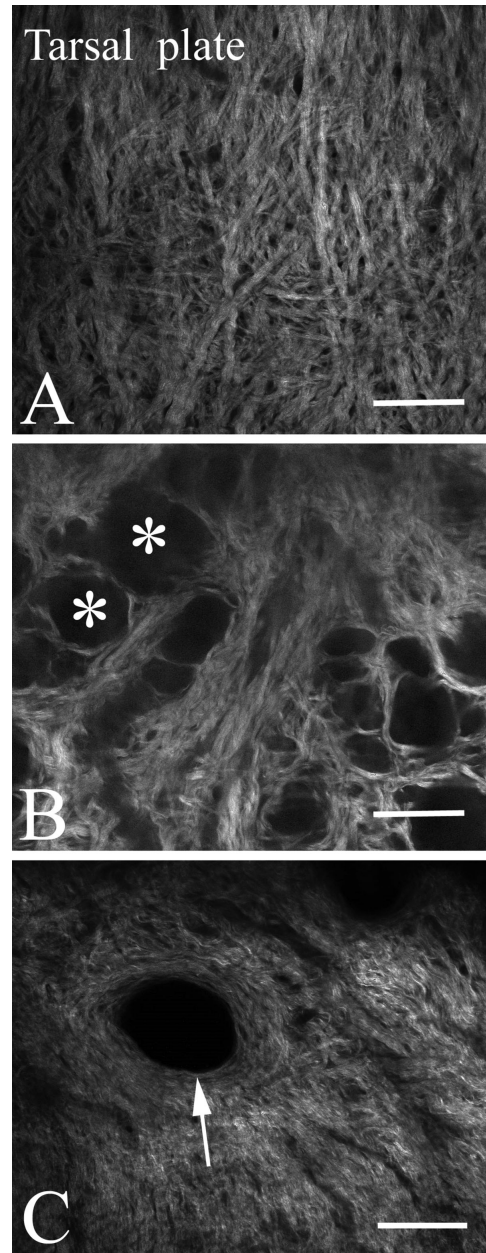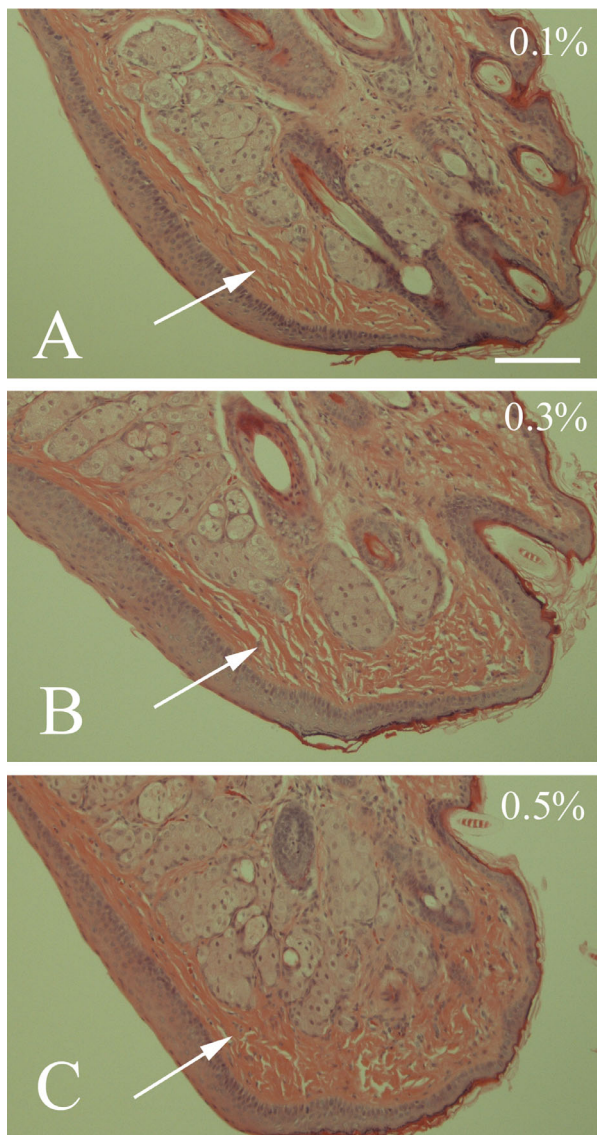
Figure 6. Histopathology images showing the effects of different riboflavin concentrations after UV-A irradiation. At 0.1% (A, *arrow*) and 0.3% (B, *arrow*), collagen bundles do not show any changes versus the control group in Figure 4. However, at the 0.5% concentration (C), connective tissue appears more compact (*arrow*). Hematoxylin and eosin stain. Original magnification, 200×. *Scale bar*: 100 μm.

Histopathology After Crosslinking Tarsal Plate

Crosslinking at lower concentrations of riboflavin (0.1% or 0.3%) did not result in structural changes to the tarsus. Histopathologic analysis did not reveal any post-irradiation changes to the connective tissue organization in the tarsus plate after crosslinking with either 0.1% or 0.3% riboflavin solution (Figs. 6A, 6B) compared to control (Fig. 4). However, crosslinking with the 0.5% riboflavin solution resulted in a more

densely packed and compact tarsal plate (Fig. 6C, arrow). All tissue samples in each group showed similar effects, with mild variability.

SHG and FRAP Study After Crosslinking

After crosslinking, tarsal plates were visualized with SHG imaging (Fig. 7). Using quantitative analysis of collagen fiber waviness (technique demonstrated in Fig. 3), collagen bundles became wavier only after treatment with the 0.5% riboflavin concentration group, but not in the 0.1% and 0.3% riboflavin groups. The 0.5% riboflavin group showed a statistically significant increase in waviness compared to the control group ($P = 0.001$) (Fig. 8). This confirms the structural changes visualized via histopathology (Fig. 6). These same SHG images were used for FRAP analysis to calculate the half-time of fluorescence recovery ($t_{1/2}$) as a measure of permeability. Again, only the tarsal plates treated with 0.5% riboflavin showed a significant decrease in $t_{1/2}$ of 3.96 seconds ($P = 0.046$) (Fig. 9), which correlates with a significant increase in tissue stiffness. This was seen across all plates.

Discussion

Currently, the sole available treatment for floppy eyelid syndrome is horizontal shortening surgery, which is typically only performed after the patient has suffered from symptoms for some period of time. Crosslinking the upper eyelid tarsus has thus garnered significant interest in the recent literature as it has the potential to become a minimally invasive procedure that could be performed long before the patient progresses to needing surgery.

Although others[3–6] have previously described methodologies for crosslinking tarsus, we are, to the best of our knowledge, the first to use SHG microscopy to study collagen fiber changes after CXL in the tarsus. This also has the advantage of not requiring delicate tissues to be stained or fixed, processes that are known to alter the cellular nanostructure.[10] Using this technique, we found that treating the tarsus with a higher concentration of riboflavin (0.5%) and 365-nm UV-A radiation for 30 minutes (total irradiance 0.45 mW/cm^2) resulted in measurable increased waviness of collagen fibers (Fig. 9). Correspondingly, histopathology studies showed a distinctly more compact structure. Treatments using lower concentrations of riboflavin with otherwise identical parameters did not result in significant structural changes. This contrasts directly with the studies done by
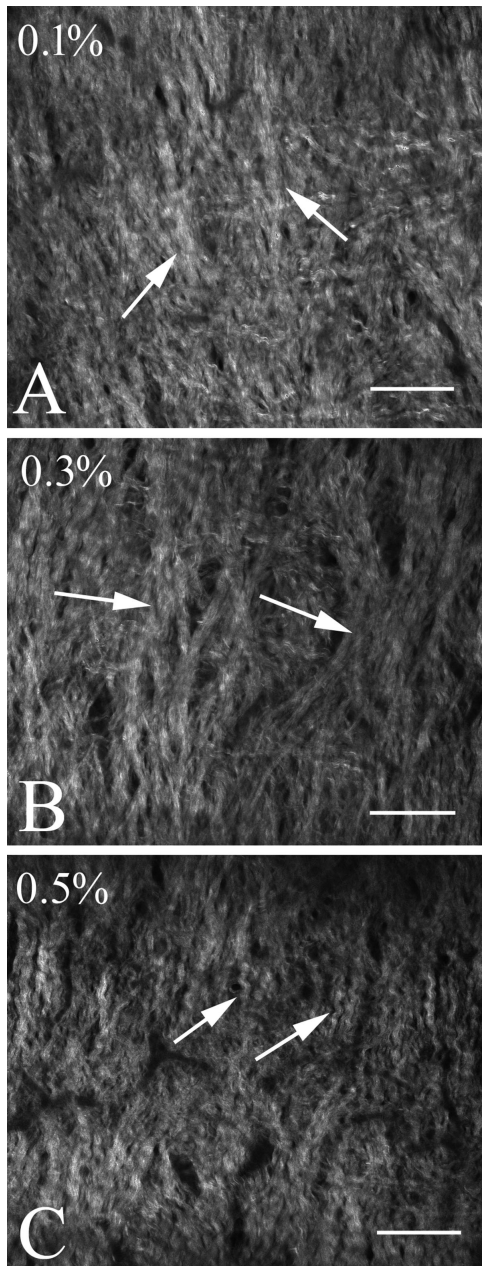
Figure 7. SHG images of tarsal collagen after crosslinking with different riboflavin concentrations. Tarsus crosslinked with 0.1% (A) and 0.3% (B) riboflavin showed collagen arrangements very similar to that of normal tarsus in Figure 5A (*arrows*). (C) After crosslinking with 0.5% riboflavin, the tarsal collagen (*arrows*) became wavier and more tightly packed. Waviness was calculated using the technique shown in Figure 3 and quantified in Figure 8. All photographs were taken at a comparable region of the tarsus at the same magnification at a depth of 30 µm. *Scale bar*: 100 µm.

Smith et al.,[3] who did not find any histopathological changes in crosslinked sheep tarsus despite reporting significant increases in tensile load. It remains to be seen whether histopathological changes are more indicative of long-term, sustainable increases in tissue stiffness.

In lieu of mechanical tensile strength testing, the FRAP technique was chosen in order to allow the study of subtle changes in tissue permeability ex vivo. In agreement with SHG and histopathology, the FRAP assay again showed that only tarsus treated with 0.5% riboflavin showed a significant decrease in permeability. From prior work using the FRAP assay in mouse peripapillary sclera, it can be extrapolated with reasonable certainty that a decrease in permeability corresponds to an increase in tissue stiffness.[11,12]

A review of previously published literature on tarsus CXL suggests that the tarsus can indeed be stiffened by irradiation, in agreement with the findings in this study.[6] However, every group differs significantly on the parameters used, particularly the riboflavin concentration, length of irradiation, and total energy of irradiance. For example, Smith et al.[3,4] crosslinked sheep tarsus with 0.1% riboflavin and a 365-nm light source (either mercury bulb or light-emitting diode [LED]) of 45, 50, or 75 mW/cm^2 over 3 minutes (total energy 7.2, 9, or 13.5 J/cm^2, respectively). Ugradar et al.[5] crosslinked thawed cadaveric human eyelids with 1% hypertonic riboflavin solution and a 365-nm LED power source of 6 mW/cm^2 over 18 minutes (total energy, 6.48 J/cm^2). Finally, DeParis et al.[6] crosslinked pig and human tarsus with 0.1% riboflavin and a 370-nm UV-A light (power, 8–9 mW/cm^2) over 60 minutes (total energy, 28.8–32.4 J/cm^2).

Of these methodologies, our study used by far the lowest amount of total energy output (0.81 J/cm^2) to achieve measurable crosslinking. This parameter is critical to consider when attempting to develop any clinical applications, as there are strict regulations in place regarding the exposure of humans to UV-A radiation between 180 and 400 nm.[20] Currently, the Dresden protocol utilizes an irradiance of 5.4 J/cm^2 to the cornea.[21] Our energy output is far below this level in rat tarsus tissue. Human tarsus, which is thicker than rat tarsus, will likely require higher energy levels. Still, it may be beneficial to minimize irradiance in order to prevent collateral damage to surrounding tissue, particularly Meibomian glands. It will be important for clinical models to be able to establish that damage will not occur to adjacent ocular tissues.

Most likely, the lower energy output of this study relates to either the choice of tissue (rat eyelid is thinner than sheep, porcine, or human tarsus) or the concentration of riboflavin used. We found that increasing the concentration of riboflavin (from 0.1% used in the Dresden cornea crosslinking protocol to 0.5%) allowed us to crosslink tissue with low levels of energy. Similarly, Ugradar et al.[5] achieved CXL with the second-lowest energy output (6.48 J/cm^2) and used 1% hypertonic riboflavin. Finally, it may
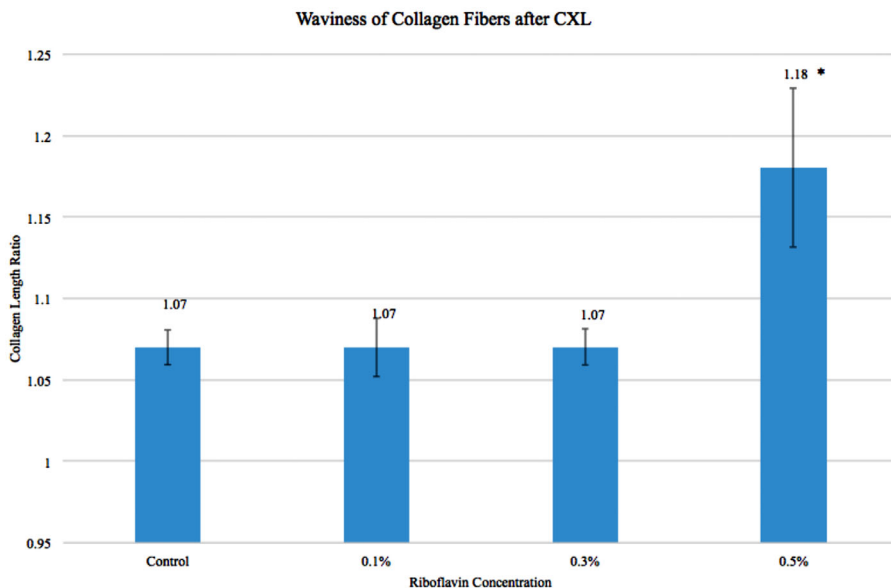
Figure 8. Waviness analysis shows an increased waviness in 0.5% riboflavin-treated tissue compared to the control group ($^*P < 0.05$). There was no statistical difference among other groups.
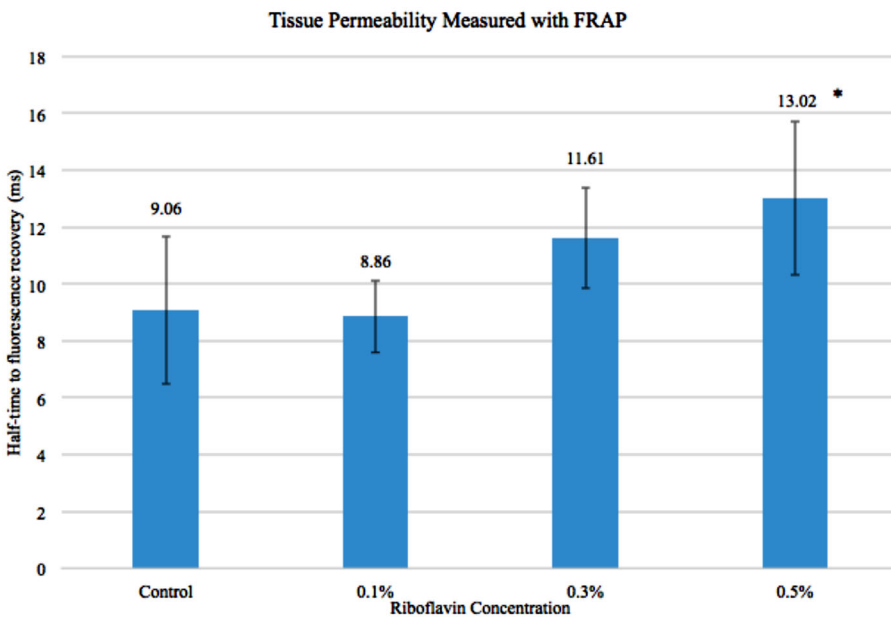

Figure 9. FRAP $t_{1/2}$ was increased in the 0.3% and 0.5% riboflavin groups and only the 0.5% riboflavin was statistically significant ($^*P < 0.05$).

also be true that crosslinking can be achieved with either combination, meaning low energy and high-concentration riboflavin are effective, as well as high energy and lower concentration riboflavin. However, one possible limitation of using a higher concentration of riboflavin is that it may limit the depth of crosslinking. If the riboflavin is highly concentrated at the surface, then this layer will absorb all of the UV-A light. On the other hand, increasing energy output to target deeper tissue could ultimately cause denaturing of surface tissue. Further studies are needed to assess if the scale and durability of crosslinking effects between these two groups are similar and which technique results in the least radiation damage to minimize the clinical side effects with lowest irradiation dose.

This study confirms a methodology by which crosslinking is achieved with low energy output and which has been confirmed with both histological studies and an indirect tissue stiffness assay. However, this study has several limitations. Although the layers of the rat eyelid are histologically similar to the human eyelid, rat tarsus is smaller and thinner than human tarsus. Tarsal tissue from larger animals or human tissue are therefore needed before we can say with certainty that crosslinking at these energy parameters is effective in human tarsus. Additionally, our histopathology studies are mainly qualitative, although they do agree with the more quantitative histology work done by Ugradar et al.[5]

Before this model can be successfully translated to an in vivo model, several questions must be answered. Foremost is the question of safety in human tissue. We suggest everting the eyelid and irradiating from the conjunctival side (as was done in this experiment). This should minimize any effects of crosslinking on eyelid tissues overlying the tarsus, as it is known from corneal studies that crosslinking only penetrates to approximately one-third the corneal depth.[22] Furthermore, altering the energy and riboflavin concentration would allow us to control the depth of effect. Ultimately, future experiments in larger species, including a primate model, are needed to determine effects on adjacent tissue and final parameters (riboflavin concentration and radiation energy level and time).

Other considerations include the amount of tarsus that must be treated before a significant effect is seen. We treated the entire length of the tarsus in the upper eyelid; the next step would be to experiment with various treatment sizes and depths in a large animal model. Finally, there may be concern over the longevity of the crosslinking effects. Extrapolating from corneal studies, we expect that tarsus crosslinking will be relatively stable and permanent.[23] We also predict that CXL can be repeated as needed to achieve the desired effect. Future in vivo studies will be necessary to assess the effect of tarsal stiffening and the long-term effects of irradiation on eyelid tissue.

Acknowledgments

* SSA and JL contributed equally to this article.

References

1. Milz S, Neufang J, Higashiyama I, Putz R, Benjamin M. An immunohistochemical study of the extracellular matrix of the tarsal plate in the upper eyelid in human beings. *J Anat*. 2005;206(1):37–45.

2. Pham TT, Perry JD. Floppy eyelid syndrome. *Curr Opin Ophthalmol*. 2007;18(5):430–4333.

3. Smith TM, Suzuki S, Cronin BG, et al. Photochemically induced crosslinking of tarsal collagen as a treatment for eyelid laxity: assessing potentiality in animal tissue. *Ophthalmic Plast Reconstr Surg*. 2018;34(5):477–482.

4. Smith TM, Suzuki S, Sabat N, et al. Further investigations on the crosslinking of tarsal collagen as a treatment for eyelid laxity: optimizing the procedure in animal tissue. *Ophthalmic Plast Reconstr Surg*. 2019;35(6):600–603.

5. Ugradar S, Le A, Lesgart M, Goldberg RA, Rootman D, Demer JL. Biomechanical and morphologic effects of collagen cross-linking in human tarsus. *Transl Vis Sci Technol*. 2019;8(6):25.

6. DeParis SW, Zhu AY, Majmudar S, et al. Effects of collagen crosslinking on porcine and human tarsal plate. *BMC Ophthalmology*. 2019;19(1):255.

7. Netland PA, Sugrue SP, Albert DM, Shore JW. Histopathologic features of the floppy eyelid syndrome. Involvement of tarsal elastin. *Ophthalmology*. 1994;101(1):174–181.

8. Ezra DG, Ellis JS, Gaughan C, et al. Changes in tarsal plate fibrillar collagens and elastic fibre phenotype in floppy eyelid syndrome. *Clin Exp Ophthalmol*. 2011;39(6):564–571.

9. Zyablitskaya M, Takaoka A, Munteanu EL, Nagasaki T, Trokel SL, Paik DC. Evaluation of therapeutic tissue crosslinking (TXL) for myopia using second harmonic generation signal microscopy in rabbit sclera. *Invest Ophthalmol Vis Sci*. 2017;58(1):21–29.

10. Li Y, Almassalha LM, Chandler JE, et al. The effects of chemical fixation on the cellular nanostructure. *Exp Cell Res*. 2017;358(2):253–259.

11. Kimball EC, Nguyen C, Steinhart MR, et al. Experimental scleral cross-linking increases glaucoma damage in a mouse model. *Exp Eye Res*. 2014;128:129–140.

12. Pease ME, Oglesby EN, Cone-Kimball E, et al. Scleral permeability varies by mouse strain and is decreased by chronic experimental glaucoma. *Invest Ophthalmol Vis Sci*. 2014;55(4):2564–2573.

13. Gao B, Yu Q, Xie F, et al. An anatomical murine model of heterotopic periorbital subunit transplantation. *Ophthalmic Plast Reconstr Surg*. 2017;33(5):367–371.

14. Marando CM, Park CY, Liao JA, Lee JK, Chuck RS. Revisiting the cornea and trabecular meshwork junction with 2-photon excitation fluorescence microscopy. *Cornea*. 2017;36(6):704–711.

15. Park CY, Lee JK, Kahook MY, Schultz JS, Zhang C, Chuck RS. Revisiting ciliary muscle tendons and their connections with the trabecular meshwork by two photon excitation microscopic imaging. *Invest Ophthalmol Vis Sci*. 2016;57(3):1096–1105.

16. Park CY, Lee JK, Chuck RS. Second harmonic generation imaging analysis of collagen arrangement in human cornea. *Invest Ophthalmol Vis Sci*. 2015;56(9):5622–5629.

17. Axelrod D, Koppel DE, Schlessinger J, Elson E, Webb WW. Mobility measurement by analysis of fluorescence photobleaching recovery kinetics. *Biophys J*. 1976;16(9):1055–1069.

18. Bradford SM, Mikula ER, Juhasz T, Brown DJ, Jester JV. Collagen fiber crimping following in vivo UVA-induced corneal crosslinking. *Exp Eye Res*. 2018;177:173–180.

19. Guo P, Miao Y, Jing Y, et al. Changes in collagen structure and permeability of rat and human sclera after crosslinking. *Trans Vis Sci Technol*. 2020;9(9):45.

20. Matthes R. Guidelines on limits of exposure to ultraviolet radiation of wavelengths between 180 nm and 400 nm (incoherent optical radiation). *Health Phys*. 2004;87:171–186.

21. Spoerl E, Mrochen M, Sliney D, Trokel S, Seiler T. Safety of UVA-riboflavin cross-linking of the cornea. *Cornea*. 2007;26(4):385–389.

22. Kymionis GD, Grentzelos MA, Plaka AD, et al. Correlation of the corneal collagen cross-linking demarcation line using confocal microscopy and anterior segment optical coherence tomography in keratoconic patients. *Am J Ophthalmol*. 2014;157(1):110–115.e1.

23. Caporossi A, Mazzotta C, Baiocchi S, Caporossi T. Long-term results of riboflavin ultraviolet A corneal collagen cross-linking for keratoconus in Italy: the Siena eye cross study. *Am J Ophthalmol*. 2010;149(4):585–593.

translational vision science & technology